Synthesis, Structure, and Bonding of Two Lanthanum Indium Germanides with Novel Structures and Properties

Arnold M. Guloy[†] and John D. Corbett*

Department of Chemistry and Ames Laboratory−DOE,[1] Iowa State University, Ames, Iowa 50011

Received October 25, 1995[⊗]

The new tetragonal phases La_3In_4Ge and La_3InGe are obtained from high-temperature reactions of the elements in welded Ta followed by annealing. The structures of both were established by single-crystal X-ray diffraction in tetragonal space group *I*4/*mcm* ($Z = 4$ and 16, $a = 8.5165(3)$ and $12.3083(2)$ Å, $c = 11.9024(4)$ and $16.0776(4)$ Å, respectively). La_3In_4Ge contains layers or slabs of three-connected indium built of puckered 8-rings and 4-rings, or of squashed tetrahedra ("butterflies") interlinked at all vertices, and these are separated by layers of La and isolated Ge. The phase is deficient of being a Zintl phase by three electrons per formula unit and is better described in terms of an alternate optimized and delocalized bonding picture and an open-shell metallic behavior for the In slabs. The more complex La_3InGe, isostructural with Gd_3Ga_2, is also layered. This phase contains pairs of mixed-occupancy (0.75 In, 0.25 Ge) sites separated by 3.020 Å, as well as isolated In and Ge atoms. The former appear to be fully reduced closed-shell atoms (relative to the bonded Ga dimers in Gd_3Ga_2) that are held in somewhat close proximity by cation matrix effects. The compound appears to be semiconducting and thus is a classical Zintl phase, $(La^{+3})_3In^{-5}Ge^{-4}$ in the simplest oxidation state notation. High Coulomb energies are presumably important for the nature of the bonding and the stabilities of both compounds.

Introduction

Interest in the study of Zintl (valence) compounds has increased markedly in recent years, deriving mainly from the rich structural variety shown by these compounds as well as the evident or prospective simplicity of their bonding schemes among polar intermetallic compounds.[2−5] Our efforts in the syntheses and characterizations of new polar intermetallics and Zintl phases[6] have also been extended into combinations of the rare-earth metals (R) with post transition metals and metalloids, e.g., Mg−La−Sb,[7] La−In,[8] and R−Ga.[9] Explorations of ternary and higher compounds that contain both group 13 (triel) and group 14 (tetrel or tetregen) elements were initiated as a result of the richness of structures and chemistry that have been discovered in the binary rare-earth-metal tetrelides.[10,11]

Many of the articles published on compounds of the triel metals have dealt with the ability of these electron-poorer elements to form multicenter covalent linkages in many homoatomic cluster and network phases, at first largely for gallium.[12] Recent results from this laboratory on a large family of alkali metal−indium and −thallium compounds have shed new light on the novel structures and bonding properties possible in group 13 homoatomic cluster anions, both isolated and condensed into networks.[6,13−19] Bonding in these phases is generally electron-deficient relative to classical two-center−two-electron bonding situations since there are more pairwise bonding interactions than electron pairs. However, magic (closed-shell) electron counts particular to cluster size coupled with Zintl concepts have still provided considerable success in rationalizing the structure-bonding schemes in these phases. Nonetheless, their conduction properties remain somewhat marginal relative to semiconducting expectations for classic Zintl phases.[6] We report here our initial results on a pair of ternary indium−germanium compounds with lanthanum as the electropositive partner, each of which exhibits some unusual structure and bonding features relative to other examples. The article concerns the synthesis, structure, and bonding both of a two-dimensional structure of linked four-atom "butterfly" clusters of indium in the metallic La_3In_4Ge and of the new Zintl phase La_3InGe with "nonbonded" dimers.

Experimental Section

Syntheses. The La metal was 5-9's Ames Laboratory product with the following principal impurities (ppm atomic): O, 190; N, 128; C, 34; F, 80; Fe, 7.6, It was stored and handled only in a He-atmosphere glovebox. Indium shot (Aesar, 6-9's purity) and electronic-grade germanium as chunks were used as received. Crystals of La_3In_4Ge and La_3InGe were initially obtained from errant reactions of the elements in welded Ta tubes during attempts to grow suitable single crystals of La_5Ge_3In[11] from a liquid In flux. The crystals were shiny black with gemlike morphologies and air-sensitive to the degree that powdered samples decompose in a few minutes. Hence, the products were handled only in an inert atmosphere, and the crystals for diffraction were sealed in thin-wall capillaries. After structural characterization of the two new compounds, they were both synthesized in high yields via reactions of stoichiometric mixtures of the elements within sealed

[†] Present address: Department of Chemistry, University of Houston, Houston, TX 77204-5641.

[⊗] Abstract published in *Advance ACS Abstracts,* April 1, 1996.

(1) Ames Laboratory is operated for the U.S. Department of Energy by Iowa State University under Contract No. W-7405-Eng-82. This research was supported by the Office of Basic Energy Sciences, Materials Sciences Division, DOE.

(2) von Schnering, H.-G. *Angew. Chem., Int. Ed. Engl.* **1981**, *20*, 33.
(3) Schäfer, H. *Ann. Rev. Mater. Sci*. **1985**, *15*, 1.
(4) Kauzlarich, S. *Comments Inorg. Chem*. **1988**, *10*, 75.
(5) Nesper, R. *Prog. Solid State Chem*. **1990**, *20*, 1.
(6) Corbett, J. D. In *Chemistry, Structure and Bonding of Zintl Phases and Ions*; Kauzlarich, S., Ed.; VCH: accepted.
(7) Ganguli, A. K.; Corbett, J. D. *Inorg. Chem*. **1993**, *32*, 4354.
(8) Zhao, J.-T.; Corbett, J. D. *Inorg. Chem*. **1995**, *34*, 378.
(9) Zhao, J.-T; Corbett, J. D. *J. Alloys Compd*. **1994**, *210*, 1.
(10) Guloy, A. M. Ph.D. Dissertation, Iowa State University, 1992.
(11) Guloy, A. M.; Corbett J. D. *Inorg. Chem*. **1993**, *32*, 3532.
(12) Belin, C.; Tillard Charbonnel, M. *Prog. Solid State Chem*. **1993**, *22*, 59 and references therein.
(13) Sevov, S.; Corbett, J. D. *Inorg. Chem*. **1991**, *30*, 4875.
(14) Sevov, S.; Corbett, J. D. *Inorg. Chem*. **1992**, *31*, 1895.
(15) Sevov, S.; Corbett, J. D. *J. Am. Chem. Soc*. **1993**, *115*, 9089.
(16) Sevov, S.; Corbett, J. D. *Science* **1993**, *262*, 880.
(17) Dong, Z.-C.; Corbett, J. D. *J. Am. Chem. Soc*. **1994**, *116*, 3429.
(18) Dong, Z.-C.; Corbett, J. D. *J. Am. Chem. Soc*. **1995**, *117*, 6447.
(19) Dong, Z.-C.; Corbett, J. D. *Inorg. Chem*. **1996**, *35*, 1444.

0020-1669/96/1335-2616$12.00/0

Ta containers at 1200 °C for 4−8 days in a high-temperature high-vacuum furnace followed by slow cooling to ~600 °C. All lines in their Guinier X-ray powder patterns could be indexed according to patterns calculated on the basis of the respective single-crystal refinement results, and the observed intensities also agreed well therewith. Lattice constants were refined from the pattern line measurements by a nonlinear least-squares means and with the aid of the lines of added Si (NIST) as an internal standard.

Structure Determinations. After examination of the crystals by standard oscillation and precession film photography, the two structure types were defined from room-temperature diffraction data obtained with the aid of Mo Kα radiation and an Enraf-Nonius CAD4 single-crystal diffractometer. Body-centered tetragonal cells were indicated for both La_3In_4Ge and La_3InGe by the photographs and supported by successful indexing of 25 tuned reflections from each on the diffractometer. In addition, the first 100 reflection intensities for each were collected without restriction to confirm the centering conditions. Axial photographs and systematic absences showed that the Laue class for both compounds was *I*4/*mmm* and that the space groups possible were *I*4*cm*, *I*4*c*2, and *I*4/*mcm*. Successful structural refinements proved that the highest symmetry *I*4/*mcm* was correct in each case.

All calculations in the refinement of the single-crystal data used the SDP and TEXSAN crystallographic packages.[20] Initial positional parameters were obtained by direct methods (SHELXS-76[21]). Isotropic refinement of the heavy atoms in La_3In_4Ge led to positional parameters that resemble those of an inverse Cr_5B_3-type structure, while the refined parameters in the case of La_3InGe are quite similar to those of Gd_3Ga_2.[22,23] Empirical absorption corrections (μ = 431 and 139 cm^{-1}, respectively) were originally applied to both data sets on the basis of four ψ-scans of each crystal, after which equivalent observed reflections yielded R_{ave} values of 3.9% and 4.2%, respectively. Further improvements in the absorption corrections were later made after the isotropic refinements had converged by the application of DIFABS,[24] after which R_{ave} values were 3.0% and 3.2%, respectively. Refinement of the occupancies of all atoms in La_3In_4Ge but La1 gave values between 0.96(1) (In) and 1.01(1) (Ge), which were concluded to be essentially unity. However, significant mixing of Ge into the In1 site in La_3InGe was evidenced by an unreasonably large thermal parameter with indium alone, and its occupancy variation gave 76.1(7)% In, 23.9(7)% Ge assuming the site was fully occupied. Axial and Laue cone (precession) photographs with long exposures did not reveal any superstructure or modulation along *c*, so the mixing was concluded to be random on an X-ray diffraction scale. Subsequent full refinement of the occupancies for the five atoms other than La1 and the mixed In1,Ge site resulted in values very close to unity, and they too were accordingly so fixed. SEM-EDX analysis of single crystals of the phase from the original synthesis yielded a relative composition of $La_3In_{1.02(1)}Ge_{0.98(1)}$, effectively identical to the refined diffraction results, $La_3In_{1.01(1)}Ge_{0.99(1)}$.

Final difference Fourier maps showed residual peaks of 2.7 and 3.1 e/Å^3 in La_3In_4Ge and La_3InGe, respectively, both within 1.0 Å of the lanthanum atoms, so unrealized interstitial impurities seem unlikely. Some of the data collection and refinement parameters are summarized in Table 1, and the positional parameters and bond distances are given in Tables 2 and 3, respectively. More details on the crystallographic studies as well as atom displacement parameters are given in the Supporting Information. These and structure factor data are also available from J.D.C.

Calculations. The theoretical treatments of the In_8^{10-} slab in La_3In_4Ge were performed within the extended Hückel formalism. The atomic orbital and energy parameters employed (ζ = 1.90 and 1.68 and H_{ii} = −12.60 and −6.19 eV for 5s and 5p, respectively) were as before.[13,25] 2-D calculations were done on both the idealized (equidistant) and the actual layer structure in order to consider the possibility of particularly distance-sensitive orbital interactions. Sixty and 90 k-point sets, selected in the irreducible wedge in the Brillouin zone, were used for average property data, respectively.

Table 1. Data Collection and Refinement Parameters

	La_3In_4Ge	La_3InGe
space group, Z	*I*4/*mcm* (No. 140), 4	*I*4/*mcm*, 16
cell param[a]		
a, Å	8.5165(3)	12.3083(2)
c, Å	11.9024(4)	16.0776(4)
c/a	1.3976	1.3062
V, Å^3	863.21(9)	2435.7(1)
fw	948.6	604.1
density(calcd), g·cm^{-3}	7.30	6.59
abs coeff (Mo Kα), cm^{-1}	431.8	130.9
range of transm coeff	0.81−1.21	0.72−1.41
R,[b] R_w,[c] %	3.1, 3.2	3.0, 4.1

[a] Guinier data with Si as an internal standard (λ = 1.540 562 Å). [b] $R = \sum||F_o| - |F_c||/\sum|F_o|$. [c] $R_w = [\sum w(|F_o| - |F_c|)^2/\sum w(F_o)^2]^{1/2}$; $w = \sigma_F^{-2}$.

Table 2. Positional Parameters and Isotropic Equivalent Displacement Parameters for La_3In_4Ge and La_3InGe

	site	*x*	*y*	*z*	B_{eq}[a] Å^2
			La_3In_4Ge		
La1	4a	0	0	1/4	0.80(1)
La2	8h	0.33538(5)	$x + 1/2$	0	1.42(1)
In	16l	0.14283(4)	$x + 1/2$	0.18633(5)	1.11(1)
Ge	4c	0	0	0	1.56(3)
			La_3InGe[b]		
La1	32m	0.19993(4)	0.06681(4)	0.13572(3)	1.16(2)
La2	8g	1/2	0	0.14396(7)	1.79(2)
La3	8h	0.16747(6)	$x + 1/2$	1/2	1.41(2)
In1,Ge[c]	16l	0.17525(5)	$x + 1/2$	0.29764(5)	1.00(2)
In2	4c	0	0	0	2.63(4)
Ge1	8h	0.1199(1)	$x + 1/2$	0	1.05(3)
Ge2	4a	0	0	1/4	0.70(4)

[a] $B_{eq} = (8\pi^2/3)\sum_i\sum_j U_{ij}a_i^*a_j^*\vec{a}_i\vec{a}_j$. [b] The last four sites correspond to Ga2,3,1,4, respectively, in Gd_3Ga_2.[22] [c] Refined as 76.1(7)% In, 23.9(7)% Ge.

Table 3. Important Distances (Å) in La_3In_4Ge and La_3InGe[a]

			La_3In_4Ge		
La1−In	x2	3.3625(3)	La2−Ge	x2	3.1818(2)
La1−Ge	x2	2.9756(1)	In−In	x2	2.8663(9)
La2−La2		3.965(1)			2.994(1)
La2−In		3.2089(7)			3.441(1)
La2−In	x2	3.4364(6)	In−Ge	x2	3.9562(4)
La2−In		3.7426(6)			
			La_3InGe		
La1−La1	x2	3.6693(7)	La2−La2		3.410(2)
La1−La2		3.7861(5)	La2−La3	x2	3.722(1)
La1−La3		3.9520(9)	La2−In1,Ge	x2	3.1917(9)
La1−La3		3.9674(5)	La2−In1,Ge	x2	3.926(1)
La1−In1,Ge		3.3043(8)	La2−Ge1	x2	3.117(2)
La1−In1,Ge		3.3644(8)	La3−In1,Ge	x2	3.2563(9)
La1−In1,Ge		3.5192(6)	La3−Ge1	x2	3.585(1)
La1−In2		3.3902(5)	La3−Ge1		3.701(2)
La1−Ge1		3.1790(8)	In1,Ge−In1,Ge		3.020(2)
La1−Ge2	x4	3.1792(5)			

[a] <4.0 Å

Results and Discussion

La_3In_4Ge. The space group and atom positions for La_3In_4Ge show it to be isopointal with inverse Cr_5B_3,[26,27] a structure type commonly known for its equal proportions of isolated and dimerized main-group elements (anions). This means that one group of compounds with this structure type, the alkaline-earth-metal (Ae) tetrelides (Ae_5Tt_3; Tt = Si, Ge, Sn, Pb), are

(20) Molecular Structure Corp., The Woodlands, TX, 1990.
(21) Sheldrick, G. M. SHELXS-86. Universität Göttingen, Germany, 1986.
(22) Yatsnko, S. P.; Hladyschewsky, R. E.; Sitschewitsch, O. M.; Belsky, V. K.; Semyannikov, A. A.; Hryń, Yu. N.; Yarmolyuk, Ya. P. J. *Less-Common Met*. **1986**, *115*, 17.
(23) Villars, P.; Calvert, L. D. *Pearson's Handbook of Crystallographic Data for Intermetallic Phases*, 2nd ed.; American Society for Metals International: Metals Park, OH, 1991.
(24) Walker, N.; Stuart, D. *Acta Crystallogr*. **1983**, *A39*, 158.
(25) Janiak, C.; Hoffmann, R. *J. Am. Chem. Soc*. **1990**, *112*, 5924.
(26) Bertaut, F.; Blum, P. *C. R. Acad. Sci*. **1953**, *236*, 1055.
(27) Pearson, W. B. *The Crystal Chemistry and Physics of Metals and Alloys*; Wiley-Interscience: New York, 1972; pp 3, 629.

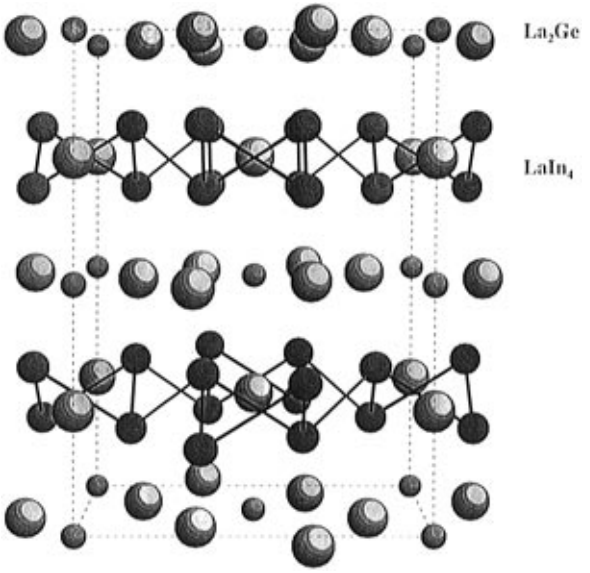

Figure 1. [100] view of the centered tetragonal structure of La_3In_4Ge ($\vec{c}$ vertical). La, In, and Ge are represented by large, medium darker, and small spheres. Note especially the puckered double In layers.

apparently electron-precise and Zintl phases [$(Ae^{+2})_5Tt_2^{-6}Tt^{-4}$ in oxidation states], although at least a few members are evidently metallic rather than semiconductors.[28] Many other compounds[23] with this structure type are stoichiometrically electron-poor and presumably metallic. In addition, the dimerization is not always observed, as in Tl_5Te_3[29] and in La_5Pb_3(O,N), an interstitial version,[30] so that a Cr_5B_3-type structural characteristic is a poor means of classification. The *c*/*a* ratios of the last two examples, 1.41 and 1.67, respectively, are also notably less than usual (1.76−1.96), and the value for the present example is every bit as small, 1.40. Furthermore, the inverse disposition of active metal and main-group elements in La_3In_4Ge and clear In−In bonding in layers put its structure quite distant from any relationship to Cr_5B_3 members as usually described.[27,29]

As shown in a [100] overview of La_3In_4Ge in Figure 1, double layers of indium (defined by Cr2 atoms in the parent) have been drawn together by ∼1 Å to generate slabs or puckered indium layers that lie normal to $\vec{c}$ and centered around $z = 0.25, 0.75$. This means the In atoms as viewed in the [001] projection of one slab in Figure 2 alternate in and out of the page in an assembly that can be described as antisymmetric pairs of 3^2434 nets 1.52 Å apart.[27,31] These can also be viewed either as puckered 8-membered rings of indium centered by La1 that are joined at every In atom via butterfly-like 4-rings and or as squashed square antiprisms and flattened tetrahedron, respectively. One of the antiprisms and a distorted tetrahedron are dashed in Figure 2, and a side view of one "tetrahedron" (or bodyless "butterfly") together with its exo connections is shown in the Synopsis (Table of Contents). The opening of opposed edges of an ideal tetrahedron has produced dihedral angles between the "wings" of 82.75° vs 109.48° otherwise and ∠(In−In−In) = 82.6°. (Equivalent but less distorted La2 tetrahedra enclose the oxygen interstitial in La_5Pb_3O.[30]) The edges of the butterfly units are 2.866(1) Å, and the interconnections between them are somewhat longer, 2.994(1) Å, while the long edges of the imagined tetrahedra (the square diagonals) are 3.441 Å. The first two correspond to very respectable In−

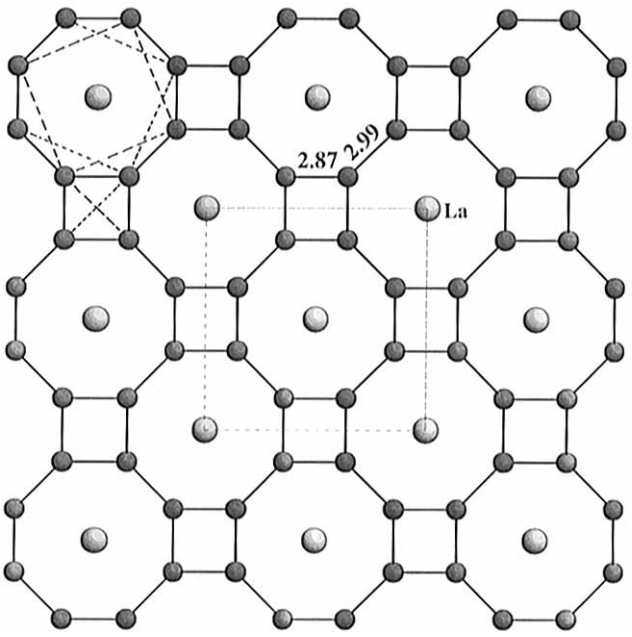

Figure 2. [001] projection of the slab of puckered 8- and 4-rings of In in La_3In_4Ge, with the former centered by La1. The In atoms are alternately displaced by 1.5 Å along the projection. This can also be described in terms of distorted tetrahedra (4-rings or butterflies), viewed with two long edges normal to the page, that are interconnected to form layers.

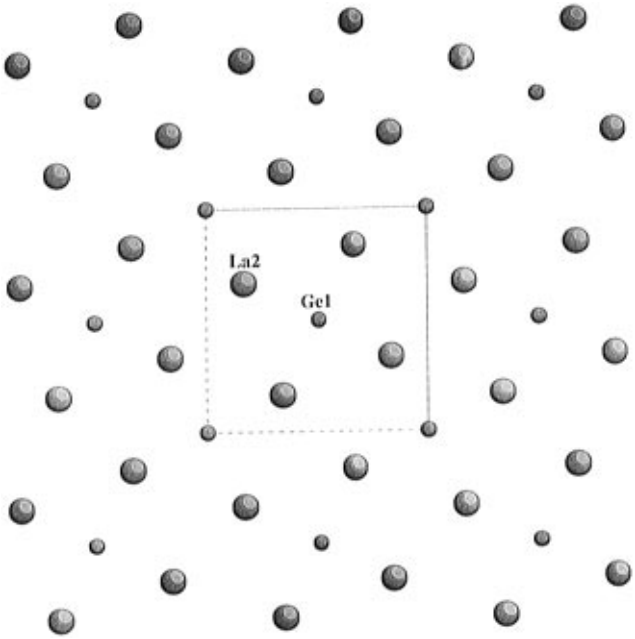

Figure 3. The La_2Ge layer that separates the In slabs (Figure 1) in La_3In_4Ge.

In bonds relative to both the Pauling single-bond distance, 2.842 Å,[32] and the many two-center intercluster bonds in the range 2.80−3.00 Å that occur in indium network structures.[13−16]

The remainder of the structure is relatively straightforward and is of less import. The indium slabs are separated by single 3^2434 nets of La2 $z = 0, 1/2$, one of which is shown in Figure 3. These are positioned such that the La2 atoms on projection along *z* virtually superimpose on the far-side members of the neighboring In slabs. Likewise, the isolated Ge atoms within La2 squares in each of these layers (Figure 3) lie directly above and below the La1 atoms that center the 8-rings, Figures 1 and

(28) Leon-Escamilla, E. A.; Corbett, J. D. Unpublished research.
(29) Schewe, I.; Böttcher, P.; von Schnering, H.-G. *Z. Kristallogr.* **1989**, *188*, 287.
(30) Guloy, A. M.; Corbett, J. D. *Z. Anorg. Allg. Chem.* **1992**, *616*, 61.
(31) The code gives the size sequence of polygons about each equivalent point in the network.
(32) Pauling, L. *The Nature of the Chemical Bond*, 3rd ed.; Cornell University Press: Ithaca, NY, 1960; p 400.

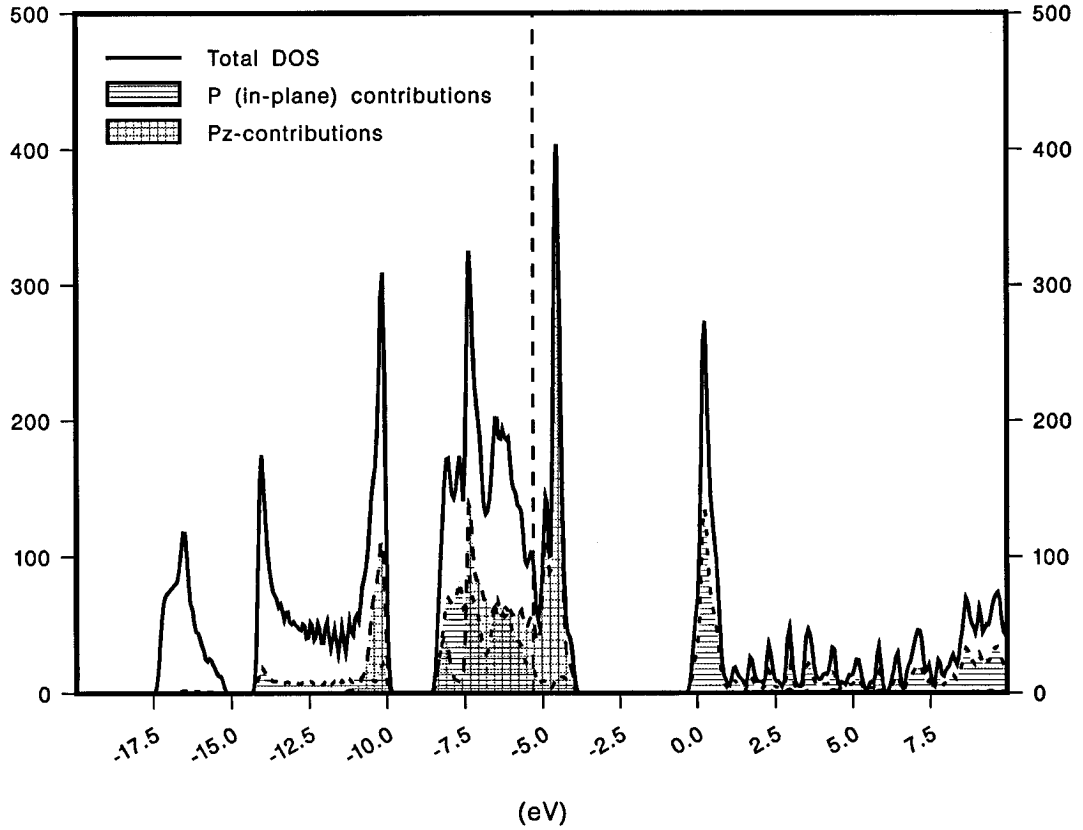

Figure 4. DOS of the In slab in La_3In_4Ge (Figure 2) according to extended Hückel calculations, with the p_z and $p_x = p_y$ contributions projected out. The dashed line marks E_F.

2. These exhibit fairly normal La−Ge distances, 2.976(1) Å to La1 (×2) and 3.182 Å to La2 (×4) compared with 2.93 Å for the (uncritical) sum of single-bond radii[32] and 3.11−3.29 Å in La_5Ge_3.[11]

Although La_3In_4Ge is closest to Tl_5Te_3[29] in terms of inverse Cr_5B_3 type structures with relatively small *c*/*a* ratios, these arrangements arise for very different reasons, and only the latter is really associated with the inverse relationship. The equivalent double Tl layers in Tl_5Te_3 are nearly 0.8 Å further apart, and there is no sense of significant Tl−Tl bonding with their 3.48 Å separations. Conversely, the noteworthy interlayer Tl−Te interactions in Tl_5Te_3 are a good deal less meaningful when these pertain to the fairly polar La−In and La−Ge contacts here.

Significantly, the new La_3In_4Ge structure does not represent a classical closed-shell bonding situation and a Zintl phase. Three-bonded (3-b) indium in the slabs would in this sense correspond to a −2 oxidation state (equivalent to a pnictogen) while isolated (0-b) germanium would be assigned a −4 oxidation state. The electron balance is thus three short ($3\cdot3 - 4\cdot2 - 4\cdot1 = -3$) for such two-center, octet assignments and a Zintl phase classification. Such a deficiency seems to be a rare event among triel compounds[6] but is found for certain alkaline-earth-metal tetrelide phases.[28] The deficit is presumably associated with the double layer $^2_\infty[In_4^{5-}]$. The same bonding result would be achieved were the isolated butterfly clusters with 12 skeletal electrons known for $Tl_2Te_2^{2-}$ [33,34] ($\hat{=} In_4^{-8}$) to be interconnected (on oxidation) by additional exo bonds at all vertices. Furthermore, the 14-e system Bi_4^{2-} with square geometry represents the reduced analog of this 13-e compound. In no sense is there any significant bonding between In slabs ($d = \geq 4.43$ Å) or of their interconnection by germanium [d(In−Ge) ≥ 3.95 Å]. There seems to be no alternative to placement of the Fermi level within the nominal valence band of the indium sheets shown in Figures 1 and 2.

Two-dimensional extended-Hückel band structure calculations on both the ideal equidistant indium layers (In−In = 2.96 Å) and the actual geometry provide some useful clarifications of the problem. The calculated DOS and COOP curves for the idealized layer show significant antibonding interactions just below E_F for the electron count In_4^{5-} (34 electrons per cell). These arise from the substantial filling of antibonding p_z orbital states (normal to the layers). We also find significant mixing of p_z with the in-plane p_x- and p_y-derived orbitals. (The s orbitals lie lower in the energy range −17.5 to −10 eV.) Bonding in the idealized structure thus would be favored at a still lower electron count near In_4^{3-}. This might be achieved via cadmium doping but has not been explored.

Calculations for the actual geometry with 0.12 Å longer intertetrahedral distances (Figure 2) show significant differences from those just described. The DOS and COOP (overlap-weighted pair population) curves, Figures 4 and 5, now have the bonding interactions (levels) fully filled at the E_F for the electron count of In_4^{5-}, while the antibonding p_z contributions have been pushed above E_F. A charge of −8 on the repeat unit, or 40 electrons per cell, would be necessary to reach the large gap shown ($E_F = -4.06$ eV).

Analysis of the different bonding interactions show that the intracluster bonding is maximized at this point while the intercluster bond levels are nearly filled. Hence, bonding interactions are maximized at the cost of the "diagonal" interaction within the flattened tetrahedra. The DOS curves indicate that the "flattening" of the ideal In_4 geometry results in a weaker mixing of antibonding p_z levels with the in-plane orbitals, optimizing the bonding within the layers. The DOS also shows that the layer is open shell and the compound, metallic. We believe that the inclusion of the remaining La and Ge atoms (ions) in the band structure will lead to broadening

(33) Burns, R. C.; Corbett, J. D. *J. Am. Chem. Soc.* **1981**, *103*, 2627.
(34) Burns, R. C.; Gillespie, R. J.; Barnes, J. A.; McGlinchey, M. J. *Inorg. Chem.* **1982**, *21*, 799.

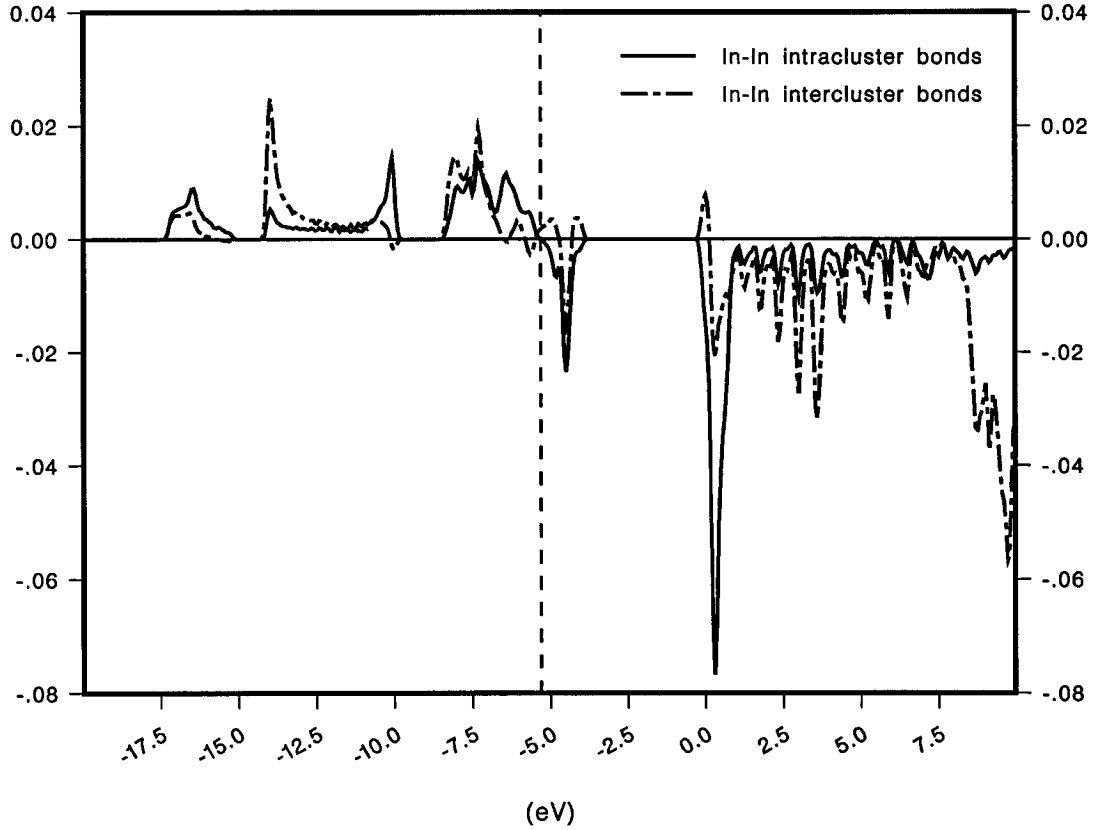

Figure 5. COOP curves for labeled In−In interactions. (Intracluster bonds are within the 4-rings.)

of the bands and result in a smaller gap between the p_z and $(p_x,p_y)^*$ bands. The Ge-derived portion of the bands are expected to lie at lower energies owing to both the lower H_{ii} of Ge and its coordination with La. However, these contributions will not significantly change the bonding picture for the In_4 layer. Clearly, compounds that are structurally Zintl phases are not always the best electronically. Presumably, the formally high charges on La and Ge entities and the Coulomb energy realized are important aspects of the stability of this unusual alternative.

We have subsequently been able to tune this array by substitution of tin for indium in the anion layer, a process which would be expected to both lower the valence band energies and increase the electron count therein. The phases $La_3In_{4-x}Sn_xGe$ for $x = 1, 2, 3$ (but not 4) have subsequently all been synthesized in high yield, illustrating the modest bonding/antibonding effects present in the band with higher filling, Figure 5. The structures for $x = 2$ and 3 have been refined to confirm that the Sn substitutes principally for In rather than Ge. The data also show that the difference in In(Sn)−In(Sn) bond lengths decrease on reduction, as expected from the calculations. The classical Zintl phase limit for this structure, La_3InSn_3Ge, is still a poor metal, but its Pauli susceptibility is only 1% of that of $La_3In_2Sn_2Ge$ ($n = 2$).[35] The size of Ge must be critical, as we have been unable to gain isostructural versions of either the ternary or the quaternary phase with either Si or Sn as the isolated atom.

La_3InGe. The unusual phase La_3InGe is isostructural but not isoelectronic with the body-centered-tetragonal Gd_3Ga_2,[22] a structure found for gallides of all but the largest trivalent rare-earth metals, namely, for Nd−Lu and Y. These compounds were once incorrectly thought to be isotypic with Zr_3Al_2 and Gd_3Al_2, which have a primitive tetragonal cell with all aluminum members dimerized.[27] The structure is a little complex, with three sites for the more electropositive metal and four for the main-group element. In La_3InGe, one of the latter has a mixed occupancy of In and Ge (essentially 3:1), while the rest contain only single-atom types (Table 2). La_3InGe evidently represents the first ternary derivative of the Gd_3Ga_2 structure type, and as an electron-richer member, it affords some unusual electronic consequences.

The structure type, which has not been described in detail before, may be constructed from alternate stacking of different 3^2434 nets, the same as encountered in La_3In_4Ge, Cr_5B_3, etc. and in the same *I*4/*mcm* space group. A composite [100] view of the layers that lie normal to *c* (ABCB′AB′CBA) is shown in Figure 6. The planar layer A at $z = 0, {}^1/_2$, shown in projection in Figure 7, is composed of two interpenetrating 3^2434 nets of La3 and Ge1 that are antisymmetric with respect to each other. The centers of the homoatomic squares, or octagons of alternating La and Ge, are occupied by In2 atoms, giving an effective La_2InGe_2 stoichiometry for layer A. The Ge1−In2 separation is >4.0 Å. Layer B at roughly $z = {}^1/_8, {}^3/_8$, etc., Figure 8, is made up of nearly coplanar La1 and La2 atoms in 4:1 proportions in a 3545 + 3535 pentagon−square−triangle net, respectively.[31] This type of network is also found in the mercury layers in Mn_2Hg_5.[36] Finally, antisymmetric pairs of B, B′ layers sandwich the important layer C, composition In_3Ge_2, around z $= {}^1/_4, {}^3/_4$. These C layers or slabs, shown in Figure 9 as the darkened In and Ge atoms, originate from the antisymmetric stacking of two 3^2434 nets of the mixed site In1,Ge (75:25) to produce twisted square antiprisms centered around (0, 0, ${}^1/_4$), etc. The Ge2 atoms (small circles) occupy the centers of, but are not bonded to, the antiprismatic In1,Ge array around (${}^1/_2$, ${}^1/_2$, *z*); instead, the pairs of B layers generate a twisted antiprism of La1 neighbors (light spheres) about Ge2. This C slab is topologically identical to the In_4 layer in La_3In_4Ge (Figure 2), but with much longer distances within the pseudotetrahedral butterfly (4.58 Å). Rather, a reduced twist within the main-group antiprisms (∼35°, Figure 9) leads instead to close In1,-Ge−In1,Ge pairs, formerly the In−In interbutterfly contacts in

(35) Harp, J. G.; Corbett, J. D. Unpublished research.

(36) de Wet, J. F. *Acta Crystallogr.* **1961**, *14*, 733.

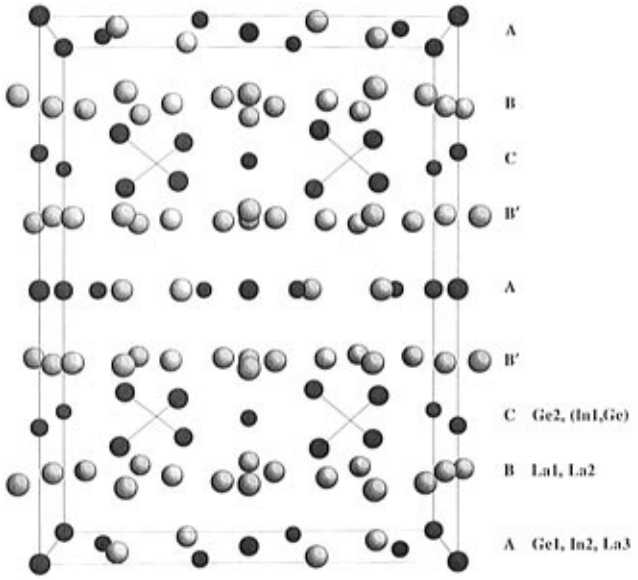

Figure 6. [100] view of the centered tetragonal unit cell of La_3InGe (distorted Gd_3Ga_2-type) with La as large light spheres and In and Ge as medium and small dark spheres, respectively ($\vec{c}$ vertical). The close-lying pairs of mixed In1,Ge (75:25) are interconnected by light lines for reference, but these atoms appear to be closed-shell and not bonded.

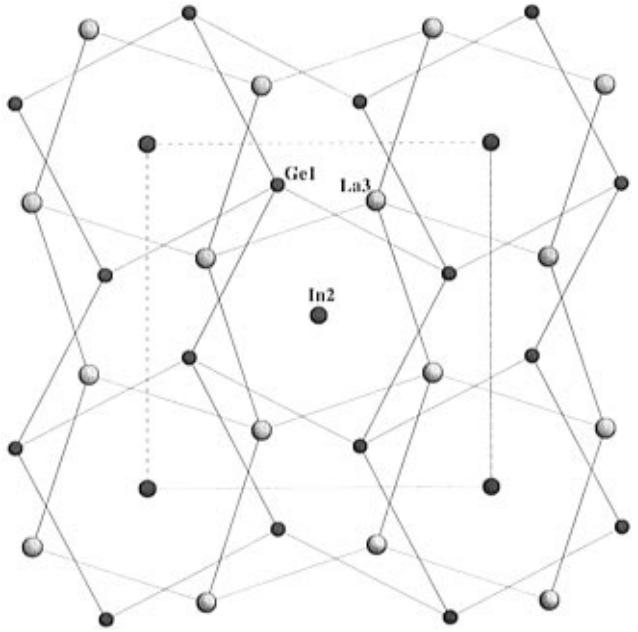

Figure 7. [001] view of the A layers at $z = 0$, $^1/_2$ in La_3InGe (see Figure 6). La3, In2, and Ge1 (in 2:1:2 proportion) are represented by light, dark, and small dark circles, respectively.

Figure 2, with separations of 3.020 Å. Note that these pairs, connected by light lines for reference, are tilted with respect to the basal plane (compare Figure 6). The mixed 75% In, 25% Ge distribution (within 2σ) is presumably responsible for the 2:1 proportion observed for U_{33}:U_{11} for the near-neighbor La2 atoms in the B layers above and below that are more or less coaxial (below). The 3.02 Å separation in these apparent In1, Ge dimers compares with single-bond distances of 2.84 Å for In−In and 2.48 Å for Ge-Ge,[32] or a population-weighted single-bond distance of 2.75 Å and a formal bond order of ca. 0.35. However, these mixed In and Ge pairs electronically appear to actually be closed-shell rather than bonded.

The B,C,B′ layer stacking seen in profile in Figure 6 also generates a short La2···La2 distance between B and B′ layers and along $\vec{c}$, 3.410(2) Å. Although this is virtually the Pauling single-bond distance, it is not significant here, as appreciable

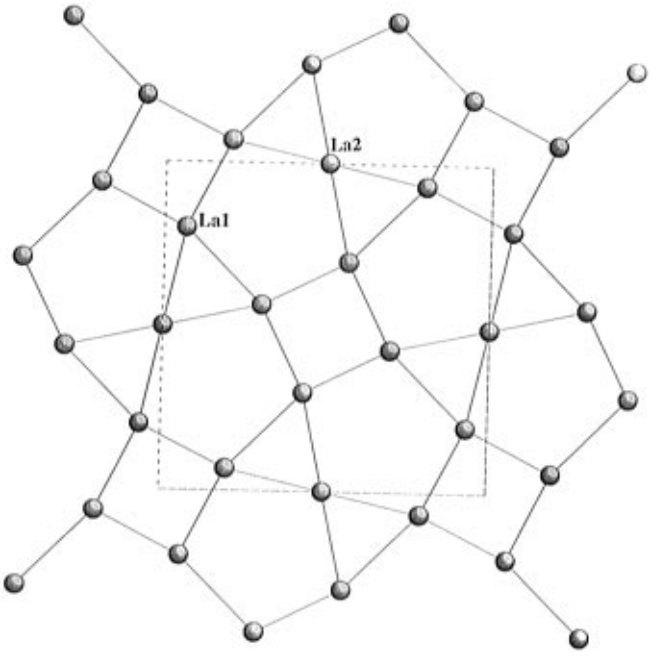

Figure 8. [001] section of the B (4La1, La2) layer in La_3InGe. The La2 atoms lie on the cell faces.

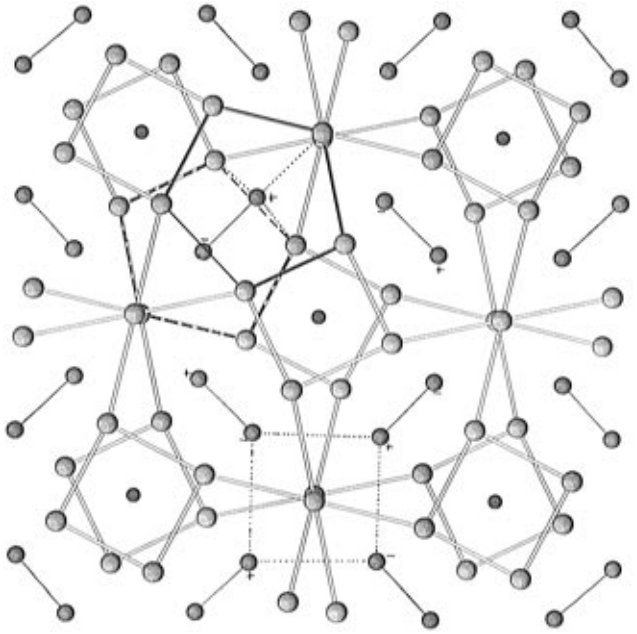

Figure 9. [001] section of a composite of the three layers B−C−B′ (Figure 6) that lie around $z = ^1/_4$, $^3/_4$ in La_3InGe. The C layer (smaller spheres) consists of Ge2 at 0, 0, $^1/_4$ and two layers of mixed In1,Ge sites that are associated in pairs. Pentagons of La2 and 4La1 from B and B′ (outlined) lie above and below these. The shortest distances about In1,Ge, 3.19 Å to La2 and 3.30 Å to La1, are dotted for one site. The (In1,Ge) tetrahedron centered by La2 that is marked in the lower region is discussed in the text.

electron transfer to In and Ge has presumably occurred, and the La2 ions are more like ion cores. These La2 pairs are seen at 0, $^1/_2$, ($^1/_4 \pm 0.144$) etc. along the S_4 axis of the well-expanded "pseudotetrahedra" formed by four In1,Ge atoms (dashed in the lower part of Figure 9). Hence, the coordination around the center is closer to a distorted octahedron—the square plane of the octahedron (In1,Ge) has been "folded" along a diagonal, and the resulting opposite corners are equidistant from the same La2. This distorted polyhedron is important in understanding the major differences between La_3InGe and the isotypic R_3Ga_2 binaries (below).

Layers of the B type also sandwich layer A, but in a

symmetrical manner that results in the effective filling of the pentagons, squares, and triangles on both B layers (Figure 8) by La3, In2, and Ge1 in A (Figure 7), respectively. Hence, La3 has a 10-fold coordination, In2, an 8-fold cubic environment, and Ge1, 6-fold within a trigonal prismatic array.

The presence of the seeming dimers of In1,Ge raises some interesting questions regarding the bonding in this potential Zintl phase, as they contradict the stoichiometry and atom distribution. La_3InGe has sufficient electrons to satisfy the oxidation state requirements of only isolated anions ($3La^{3+} + In^{-5} + Ge^{-4}$, $3 \cdot 3 - 5 - 4 = 0$). Literal realization of these assignments to the anions, even as oxidation states (not charges), is of course problematic, especially for octet indium,[6] although the higher Coulomb potentials in this phase should help. In fact, a localized (closed-shell) electronic assignment is supported by resistivity measurements on La_3InGe by the Q-method[37] which showed $\rho_{293} \sim 200\ \mu\Omega\cdot$cm and a temperature dependence of $-0.82(5)\%\ K^{-1}$ over 150−300 K, that is, semiconducting in character. Thus, the absence of metallic conduction (which says something about DOS only at E_F) appears to support a nonbonding (closed-shell) interaction within the In1,Ge pairs (which must involve two In 50% of the time); otherwise, their pairwise bonding would presumably free two electrons per dimer (16 per cell) that would fall in the conduction band unless some unusual trapping mechanism for these were to be present. In addition, it is otherwise difficult to understand why and how the electron-richer Ge would and could be incorporated into the Gd_3Ga_2 structure. Relative to Gd_3Ga_2, where the corresponding Ga2−Ga2 distance is 2.80(1) Å and is certainly bonding, precisely 16 Ge atoms per cell have been introduced into the structure in the formation of La_3InGe, 12 as the isolated Ge1 and Ge2 and four in the eight mixed dimers, and their additional valence electrons exactly eliminate the need for bonding within eight quasi-dimers. The relative size of Ge must be important in this unusual structure inasmuch as it occurs in three different sites. It should be noted that a semimetallic rather than a semiconducting behavior does not alter a closed-shell, Zintl phase assignment.

Finally, the cation distances around In1,Ge offer some support for the notion that the "dimer" results from matrix effects,[38] the crowding of each atom therein by the surrounding La atoms, especially those opposite the "bond". The two La1, La2 pentagons that fall above and below each pair of In1,Ge atoms are drawn in Figure 9 with solid and dashed lines, respectively (2-fold axes at $z = {}^1/_4$ and normal to [110] etc. bisect the In1,Ge−In1,Ge pairs). The shorter La−In1,Ge separations (dotted) are 3.192 Å to a La2 atom on the back side and 3.304 Å (×2) to a pair of La1 atoms in the other pentagon, together with 3.256 Å to La3 in the A layer, normal to the view (not shown). The other two distances to La1 are longer, 3.364 and 3.519 Å. A weighted "normal" d(La−In1,Ge) is about 3.34 Å, emphasizing how short the two 3.19 Å La2 separations are that appear to "push" the La1,Ge atoms inward and toward each other. Good theoretical modeling of La_3InGe needs to be developed to understand the bonding and properties better.

The apparent crowding of the "nonbonded dimers" $(In1,Ge)_2$ should naturally be reduced by substitution of gallium for indium. Nine gallium atoms per cell, equivalent to 75% of the indium atoms refined on this particular site, have been substituted in the isostructural $La_3In_{0.44}Ga_{0.56}Ge$, with a volume reduction of 2.6%. These do indeed substitute at this particularly small site.[39]

Some contrasts between La_3InGe and the isostructural Gd_3Ga_2 are helpful. If the short Ga−Ga separation, 2.800(8) Å, is considered bonding, then Gd_3Ga_2 too is structurally a Zintl phase: $12\ Gd^{3+} + 4Ga^{-5} + 2(Ga_2^{-8})$ in the independent unit. In fact, the isomorphous Y_3Ga_2, with smaller cations and d(Ga−Ga) = 2.791(3) Å, virtually the same as in Gd_3Ga_2 and also a classical (structural) Zintl phase, is not closed-shell electronically but Pauli-paramagnetic and metallic with $\rho_{293} \cong 40\ \mu\Omega\cdot$cm.[40] The persistence of the dimers is still significant.[6] The contrast with La_3InGe suggests that this structure type may be flexible enough to accommodate either bonded dimers or pairs of closed-shell atoms. The dimensional differences between Gd_3Ga_2 and La_3InGe are small, in spite of the obvious electronic contrasts. Although the c/a ratios are similar, 1.29 and 1.30, respectively, the B layer in Gd_3Ga_2 is significantly more buckled, the planes of the equivalent Gd1 and Gd2 atoms therein being displaced from one another by 0.23 Å compared with 0.13 Å in La_3InGe. This results in relatively shorter Gd2−Gd2 distances across the slab (B to B′), so that the distorted (interdimer) polyhedron Gd_2Ga_4 around 0, ${}^1/_2$, ${}^1/_4$ has a shorter apical separation and larger basal (interdimer) distances compared with those within the comparable $(La_2)_2(In1,Ge)_4$. (The waist of this last unit is dotted at the bottom of Figure 9 and can also be secured by adding La2 atoms above and below the puckered ring shown in the Synopsis.) The larger basal Ga−Ga distances in this Gd_2Ga_4 unit seem to be a clear consequence of dimer formation with the neighboring Ga atoms (compare Figure 2). The opposite effect in the relatively elongated $La_2(In1,Ge)_4$ polyhedra in La_3InGe from evident In1,Ge-In1Ge repulsion can be also described in terms of a greater breathing-like displacement.

Conclusions

Two new ternary lanthanum−germanium−indium phases that exhibit novel structural and bonding characteristics have been described: La_3In_4Ge and La_3InGe. To a certain degree, the Zintl concept is helpful in understanding the structure−bonding−property relationships. However, the first compound exhibits delocalized bonding in indium layers with an open band rather than a Zintl result, while the semiconducting Zintl phase La_3InGe persists with closed-shell anions in a structure type that was originally based on dimers. The apparent electronic and structural flexibilities of Cr_5B_3- and Gd_3Ga_2-type structures clearly allow the accommodation of diverse structural elements and, in essence, give us some early appreciation and understanding of the valence state tolerances of nominally metallic structure types. Interrelationships of many factors, particularly atomic size and electronic requirements, in the determination of structural preferences of polar intermetallics is shown by the many compounds isopointal with the Cr_5B_3 type. The validity of the Zintl concept, aided by close consideration of the individual structures, is widely recognized to afford some elementary understanding of the chemical bonding in many polar intermetallics. However, the degree of overlap between the metal-based and metalloid states may be a major factor in the full interpretation of the bonding in polar and semipolar intermetallics, especially when conduction criteria are included. Further investigations on classes of compounds that lie on both sides of the Zintl border should lead to a more general understanding of such novel compounds.

Supporting Information Available: Tables of additional diffraction and refinement details and of the anisotropic atom displacement parameters (2 pages). Ordering information is given on any current masthead page.

IC951378E

(37) Shinar, J.; Dehner, B.; Beaudry, B. J.; Peterson, D. T. *Phys. Rev.* **1988**, *B37*, 2066.
(38) Corbett, J. D. *J. Solid State Chem.* **1981**, *37*, 335.
(39) Henning, R. W.; Corbett, J. D. Unpublished research.
(40) Zhao, J.-T.; Corbett, J. D. Unpublished research.